

# The Influence of Poly-(L-Lysine) and Porin on the Domain Structure of Mixed Vesicles Composed of Lipopolysaccharide and Phospholipid: An Infrared Spectroscopic Study

Peter Lasch, Christian P. Schultz, and Dieter Naumann

Robert Koch-Institut, 13353 Berlin, Germany

**ABSTRACT** Fourier transform infrared (FTIR) spectroscopy has been used to study the thermotropic phase behavior of binary lipid mixtures composed of deuterated phospholipids (PLs) and lipopolysaccharides (LPSs). Furthermore, the influence of an extrinsic high-molecular, polycationic polypeptide (poly-(L-lysine), PLL<sub>(500)</sub>) and an intrinsic membrane protein (outer membrane protein F, OmpF) on these binary mixtures was investigated by FTIR spectroscopy. “Deep rough” mutant LPS (ReLPS), isolated from *Salmonella minnesota R595*, and perdeuterated 1,2-dimyristoylphosphatidylethanolamine (DMPE<sub>d54</sub>) were used as model lipids. Deuteration of one of the lipids permitted the detection of lipid-protein interaction with each lipid component separately. For this purpose, the symmetric  $>CH_2$  and  $>CD_2$  stretching bands were utilized as specific monitors to scrutinize the state of order of the membranes. From the individual phase transition temperatures  $T_m$  and the shape of the phase transition profiles, it is established that ReLPS and DMPE<sub>d54</sub> are molecularly immiscible. In addition to the two domains of the pure lipid components, a third, domain-like structure is detected that may coexist with these pure domains. This domain-like structure undergoes a gel to liquid-crystalline  $L_1$  ( $\beta \leftrightarrow \alpha$ ) phase transition at temperatures distinctly different from that of the respective pure lipid domains. The nature of this type of domain is discussed in terms of a “border region” model that adequately explains the experimentally observed complex phase transition profiles. It is further demonstrated that the extrinsic polycationic polypeptide PLL<sub>(500)</sub> and the intrinsic, pore-forming protein OmpF isolated from *Escherichia coli* interact preferentially and highly specifically with the negatively charged ReLPS. Both the synthetic polypeptide and the pore-forming protein increased the tendency of ReLPS and DMPE<sub>d54</sub> to segregate into distinct, well-separated domains. Whereas the transition profiles of the ternary system ReLPS/DMPE<sub>d54</sub>/PLL<sub>(500)</sub> showed the features of a phase segregation phenomenon not affecting the transition temperatures of the pure lipid components, the ternary system composed of ReLPS/DMPE<sub>d54</sub> and OmpF exhibited phase transition curves that were characterized by an unspecific (DMPE<sub>d54</sub>/OmpF) and a strong and unique (ReLPS/OmpF) type of lipid-protein interaction. Furthermore, semiquantitative estimations supported the supposition that OmpF might be able to induce bilayer asymmetry in preformed symmetrical ReLPS/DMPE<sub>d54</sub> vesicles.

## INTRODUCTION

Gram-negative bacteria contain, besides the cytoplasmatic membrane and the murein layer, an additional barrier, the outer membrane (OM), which plays an important role in bacterial antibiotic resistance, regulation of nutrient and waste product exchange, and protection against proteolytic enzymes, bile and bile salts, or other biologically active substances. It is well known that the outer membrane is made up of two different leaflets, one outer sheet formed exclusively by lipopolysaccharides (LPSs), and an inner layer composed mostly of phosphatidylethanolamines (80%) and phosphatidylglycerols (~15%) (Kamio and Nikaido, 1976; Nikaido and Vaara, 1985). In this asymmetrical bilayer, channel-forming proteins (porins) are embedded, which allow hydrophilic molecules of less than 600 Da to cross the OM. Lipopolysaccharides are only found in the OM of Gram-negative bacteria and are responsible for many immunological reactions in host organisms during infection (Rietschel and Brade, 1992; Rietschel et al., 1994; Schletter

et al., 1995). These LPSs consist of a poly- or oligosaccharide portion and a negatively charged, so-called core region that is covalently linked to a lipid moiety, the lipid A, which anchors the LPS in the outer membrane and represents the “endotoxic principle” of LPS. The molecular assembly of LPS is thought to be responsible for the barrier function of the OM toward a variety of important hydrophobic drugs, because of its ability to form highly ordered structures and strongly interacting complexes with porins and divalent cations (Rottem and Leive, 1977; Nikaido and Vaara, 1985; Labischinski, 1985). It has become evident from several experiments that the outer leaflet of the OM of deep rough mutants, which produce minimal LPS structures, contains besides LPS small amounts of phospholipids (Kamio and Nikaido, 1976; Nikaido, 1979; Nikaido and Vaara, 1985). It has been extensively discussed that the known higher sensitivity of these LPS mutant strains to various hydrophobic drugs is due to lateral phase segregation phenomena and the formation of stable phospholipid domains in the outer layer of the OM, which allow the hydrophobic molecules to penetrate (Takeuchi and Nikaido, 1981; Vaara and Vaara, 1983b; Nikaido, 1990). To influence the permeation properties of the OM, divalent cations and polycationic molecules like, e.g.,  $Ca^{2+}$ , high-molecular-weight poly-(L-lysine), and polymyxin nonapeptide (PMBN) have been used

Received for publication 19 May 1997 and in final form 8 May 1998.

Address reprint requests to Dr. Dieter Naumann, Robert Koch-Institut, Nordufer 20, D-13353 Berlin. Tel.: +49-30-4547-2259; Fax: +49-30-4547-2606; E-mail: NaumannD@rki.de.

© 1998 by the Biophysical Society

0006-3495/98/08/840/13 \$2.00

as membrane-active substances (Jones and Osborn, 1977; Vaara and Vaara, 1983a; Marvin et al., 1989). The treatment of smooth (wild-type) strains of Gram-negative bacteria with polycations causes the release of 20–30% LPS from the OM and, at the same time, drastically increases its permeability to hydrophobic antibiotics (Vaara and Vaara, 1983b). In view of these data, a gradual depletion of LPS molecules beyond a critical level, causing phospholipids (PL) to appear in the outer leaflet of the OM to compensate for the loss of LPS from the cells, was discussed. Such PL patches are thought to be present in the outer leaflet of the OM smooth strains after treatment and to be characteristic of deep rough mutants. The passage of hydrophobic agents through the OM may take place at these symmetrical PL domains.

To characterize the nature of LPS interaction and the lateral domain organization of LPS/PE mixtures, Langmuir-Blodgett measurements were performed (Fried and Rothfield, 1978). From these studies it was concluded that one LPS molecule and 16 molecules of PE may form a tight stoichiometric complex constituting molecularly mixed domains. These findings were found to be diametrically opposite to considerations based on electron spin resonance measurements of LPS and spin-labeled phospholipid (PE) mixtures (Takeuchi and Nikaido, 1981). The authors stated that LPS and PE tend to persist in separate lipid domains, even in the presence of porin and  $\text{Ca}^{2+}$ . Modern Fourier transform infrared spectroscopy (FTIR) provides an easy-to-use and structure-sensitive methodology for the investigation of complex systems like ternary mixtures of lipopolysaccharide/perdeuterated 1,2-dimyristoylphosphatidylethanolamine (LPS/DMPE<sub>d54</sub>) and outer membrane protein F (OmpF), with the additional advantage of avoiding the use of potentially perturbing probe molecules. Thus, to characterize the presumed highly specific LPS/OmpF interactions and to test the “phospholipid domain” hypothesis, binary mixtures of deep rough mutant LPS (ReLPS) from *S. minnesota* and perdeuterated DMPE<sub>d54</sub>, and the influence of the intrinsic, pore-forming protein OmpF from *E. coli* and the extrinsic, high-molecular poly(L-lysine) polypeptide on the domain organization of these binary lipid mixtures were investigated by FTIR spectroscopy. The wealth of structural information obtained is discussed in terms of structure and permeability properties of the OM.

## MATERIALS AND METHODS

### Materials

Dimyristoylphosphatidylcholine (DMPC) and poly(L-lysine) with 500 lysine residues (PLL<sub>(500)</sub>) were purchased from Sigma (Deisenhofen, Germany). The deuterated phospholipid DMPE<sub>d54</sub> was obtained from Avanti Polar Lipids (Birmingham, AL) and was used without further purification. Before preparation of the binary mixtures,  $T_m$  and  $\Delta H_m$  values of the fully hydrated pure ReLPS and DMPE<sub>d54</sub> membrane vesicles were determined by FTIR. From the literature it is known (Petersen et al., 1975) that perdeuteration of the acyl chains of phospholipids generally causes a 4–5 K decrease in phase transition temperature. Furthermore, it is known that the use of D<sub>2</sub>O solutions causes an upshift in the main phase transition

temperatures  $T_m$  of ~0.2–0.4 K (Casal and Mantsch, 1984). For DMPE<sub>d54</sub>, a  $T_m$  of ~46.2°C was observed, in good agreement with the literature data (49.5°C for DMPE in H<sub>2</sub>O; Mabrey and Sturtevant, 1976).

For all experiments, ReLPS isolated from deep rough mutant R595 of *Salmonella minnesota* was used. For LPS isolation, the cells of this strain were grown at 37°C, and the LPS was isolated and purified according to the phenol/chloroform/light petrol ether extraction procedure described by Galanos and Lüderitz (1975). Only electrodyalyzed samples of the Na<sup>+</sup> salt form of ReLPS, absolutely devoid of the divalent cations Ca<sup>2+</sup> and Mg<sup>2+</sup>, were used for FT-IR analysis. The gel to liquid crystalline phase transition temperature  $T_m$  of pure ReLPS dispersions in D<sub>2</sub>O was determined by FTIR at 26.1°C, a value corresponding well with earlier findings (Naumann et al., 1989). OmpF porin from *E. coli* K12 (Garavito and Rosenbusch, 1986) was a generous gift from J. P. Rosenbusch (Biozentrum Basel).

### Sample preparation

To obtain fully hydrated vesicles of the binary mixtures, the desired amounts of DMPE<sub>d54</sub> and ReLPS (or DMPE<sub>d54</sub> and DMPC) were first dissolved in a chloroform-methanol-water mixture (83/15/2 vol%) and were subsequently sonicated for 15 min (Sonorex RK100; Bandelin GmbH, Berlin, Germany) at the minimum power setting. The solvent was then removed by evacuation for an overnight period. After dispersion in a D<sub>2</sub>O buffer (pD at 7.2), the lipid mixtures were again sonicated for 15 min at temperatures above the main phase transition of both lipid components (50°C). Subsequently, the lipid dispersions were quickly frozen in liquid nitrogen and slowly thawed. This cycle was repeated three times.

To obtain lipid dispersions suitable for FTIR measurements, the samples were pelleted by centrifugation (Beckman Airfuge; Beckman Instruments, Munich; 80,000 × g, 30 min) and prepared as gel films between two CaF<sub>2</sub> windows with spacers of 50 μm. Further “annealing” of the samples was achieved directly in the IR cuvette by applying three repeating temperature cycles (4°C → 70°C → 4°C) to guarantee complete equilibration of the samples. The equilibration process was checked by FTIR spectroscopy from the conformity of successive up- and down-scan phase transition profiles.

OmpF was integrated in the mixed lipid vesicles by applying three freeze-thaw cycles in the presence of the protein, followed by annealing cycles until equilibration was reached. To remove the detergent octylpolyoxyethylene (o-POE), the proteoliposomes were then dialyzed against 20 mM EDTA buffer for 72 h. No denaturation of the protein after these treatments was detected using the constancy of the structure-sensitive amide I band contour as a criterion.

The integration of OmpF into the liposomes was assessed by FTIR linear dichroic measurements, in accordance with a method described by Rothschild (Rothschild and Clark, 1979). The dichroic ratios were determined for the amide I band at 1630 cm<sup>-1</sup> and the amide II band near 1550 cm<sup>-1</sup> (data not shown). Orientation parameters obtained for the β-sheets of the porin relative to the membrane normal (49°) were found to be in a good agreement with results (47°) published by Nabedryk and co-workers (Nabedryk et al., 1988).

For further data analysis, the molar ratios of ReLPS and DMPE<sub>d54</sub> (binary mixtures) and of ReLPS and OmpF (ternary mixtures) were determined using the integral intensities of the symmetrical >CH<sub>2</sub> stretching band at 2850 cm<sup>-1</sup> (for ReLPS), the >CD<sub>2</sub> stretching band at 2089 cm<sup>-1</sup> (for DMPE<sub>d54</sub>), and the tyrosine ring vibration band at 1515 cm<sup>-1</sup> (for OmpF) as internal standards.

### Experimental design, FTIR data acquisition, and evaluation

The membrane samples were sealed in a gas-tight IR cuvette cartouche, which was placed in a thermostatted metal jacket. The temperature was controlled by a programmable temperature bath (Haake 3C; purchased from Haake Karlsruhe, Germany). For precise temperature measurements,

a thermocouple connected to a Testotherm thermometer (Testo, Lenzkirch, Germany) was placed in a bore of the IR window near the sample. Spectra were recorded on an IFS-66 FTIR spectrometer (Bruker Analytische Messtechnik GmbH, Karlsruhe, Germany), equipped with a water-cooled globar and a deuterated triglycine sulfate (DTGS) detector. The nominal spectral resolution used was  $4\text{ cm}^{-1}$ . One hundred ten scans were coadded per sample spectrum and were apodized using a trapezoidal four-point apodization function for Fourier transformation. Interferograms were zero-filled, using a zero filling factor of 4 to yield an encoding interval of approximately one data point per wavenumber. Typically, a linear temperature gradient of  $0.25\text{ K/min}$  with two repeating temperature cycles from  $5^\circ\text{C} \rightarrow 80^\circ\text{C} \rightarrow 5^\circ\text{C}$  was applied for temperature profile measurements. Effectively, one averaged FTIR spectrum was collected and stored per  $0.5\text{ K}$  temperature increase/decrease.

Mathematical operations on the spectra (Fourier transformation, water vapor subtraction, baseline correction, determination of peak parameters) were accomplished using the OPUS 2.0 software package from Bruker and a macrointerpreter of the Bruker IR software package. Briefly, spectra of the lipid mixtures were base line subtracted in the  $3000\text{--}2800$  and  $2200\text{--}2000\text{ cm}^{-1}$  regions. Subsequently, the peak parameters (band position, intensity, and half-width) of the  $\nu_{\text{sy}}(>\text{CH}_2)$  and  $\nu_{\text{sy}}(>\text{CD}_2)$  bands were determined using the peak picking routines of the Bruker software package. The  $\theta$ -profiles (cf. Appendix) were calculated with self-written software, and they were fitted with the software package Origin 4.0 (MicroCal Software, Northampton, MA).

## RESULTS

### The strategy for analyzing lipid mixtures

Dispersions of many bilayer-forming amphiphiles (e.g., phospholipids, sphingolipids, lipopolysaccharides) show a remarkably complex thermotropic polymorphism. The acyl chain melting phase transition of lipid bilayers, the so-called gel to liquid-crystalline phase transition (e.g., the  $L_\beta \leftrightarrow L_\alpha$  phase transition of lamellar bilayer structures according to the nomenclature of Luzzati (Tardieu and Luzzati, 1973)) involves the introduction of conformational disorder (i.e., *gauche* rotamers in the acyl chains) and conformational rearrangements in the interfacial and polar headgroup regions, which, in turn, lead to considerable changes in the infrared spectrum of the given amphiphiles. IR bands observed in the  $3000\text{--}2800\text{ cm}^{-1}$  region, which arise predominantly from the symmetrical and asymmetrical  $>\text{CH}_2$  and  $>\text{CH}_3$  stretching vibrations, are known to be sensitive to temperature-induced changes, and it is well established that the frequency, the intensity, and the width of these bands specifically monitor the membrane state of order and the motional freedom of the methylene groups (for a review see Casal and Mantsch, 1984). Lipids with fully deuterated acyl chains show the  $>\text{CD}_2$  stretching bands between  $2050$  and  $2200$  wave numbers, well separated from the C-H stretching region. Because they are overlapped less by other vibrational modes, only the symmetrical  $>\text{CH}_2$  and  $>\text{CD}_2$  stretching modes were used in this study to analyze the thermotropic phase behavior.

The strategy for elucidating the phase behavior of binary mixtures of lipids by vibrational spectroscopy and obtaining information on phase separation processes at the molecular level is generally to investigate the mixed membranes, in which one of the lipid components is deuterated. This makes

it possible to detect membrane order parameters of an individual component in a multicomponent system in a single experiment (Dluhy et al., 1983; Casal and Mantsch, 1984; Kouaouci et al., 1985).

FTIR spectra of a lipid mixture of ReLPS and  $\text{DMPE}_{\text{d}54}$  recorded at different temperatures during a typical heating run are shown in Fig. 1. Quite obviously, all of the C-H and C-D stretching bands change abruptly in frequency, intensity, and width in the phase transition region, indicating a decrease in conformational order with increasing temperature.

The experimentally available frequency/temperature profiles of the symmetrical stretching band of  $>\text{CH}_2$  and  $>\text{CD}_2$  exhibit a nonlinear functional relationship to the temperature dependence of the fraction of melted lipids  $\theta(T)$ . Thus only  $\theta(T)$  profiles have to be used to obtain

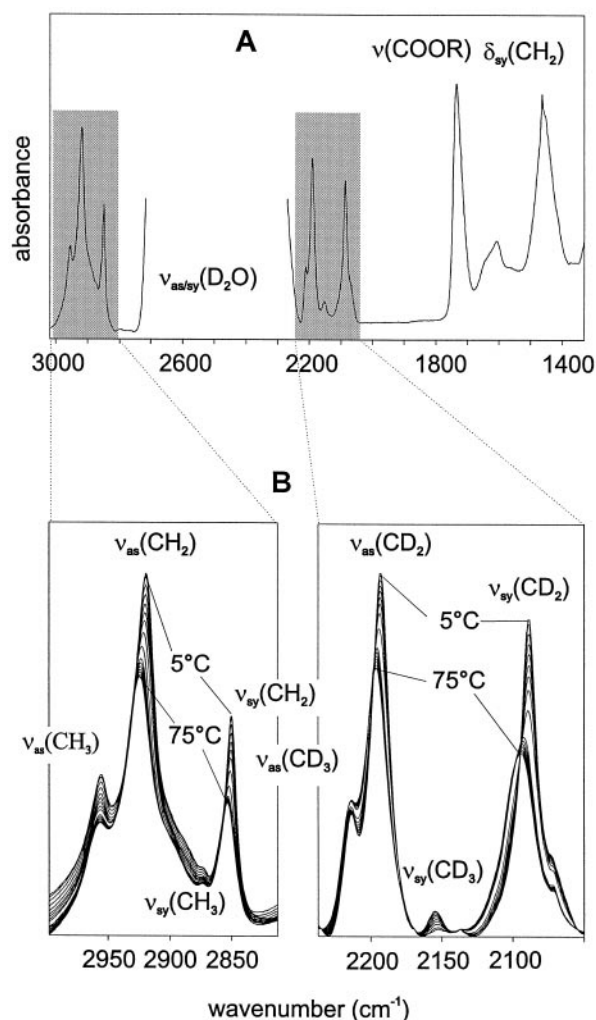


FIGURE 1 Typical FTIR spectra obtained from a fully hydrated lipid dispersion of a binary mixture composed of ReLPS and deuterated  $\text{DMPE}_{\text{d}54}$ . (A) A survey spectrum in the  $1300\text{--}3000\text{ cm}^{-1}$  region. (B) Series of FTIR spectra in the  $>\text{CH}_2$  and  $>\text{CD}_2$  stretching region collected at different temperatures of a typical heating run. Phase transitions, particularly sharp for the  $\text{DMPE}_{\text{d}54}$  component, are evident from abrupt peak shifts to higher values, the increase in bandwidths, and the decrease in band intensities.

reliable thermodynamic parameters such as the midpoint phase transition temperature  $T_m$  and the van't Hoff enthalpy  $\Delta H_m$  of the transition. The description of the model used to generate these  $\theta(T)$  phase transition profiles and to determine the  $T_m$  and  $\Delta T_m$  values is given in the Appendix.

### Binary lipid mixtures

For legibility, only some of the experimentally determined frequency/temperature profiles of the ReLPS and DMPE<sub>d54</sub> component in binary lipid mixtures are depicted in Fig. 2. From these curves it is evident that the ReLPS transition profiles change systematically to higher temperatures with increasing portions of DMPE<sub>d54</sub> (vice versa for the DMPE<sub>d54</sub> profiles). From the shape of the transition profiles shown in Fig. 2, it can also be seen that the phase behaviors of the ReLPS and DMPE<sub>d54</sub> components give rise to at least two different transitions. This can be visualized by calculating the first derivatives of the experimental frequency/temperature profiles. As an illustration, Fig. 3 shows the first derivatives of the experimental frequency/temperature plots of a binary mixture of DMPC and DMPE<sub>d54</sub> in an equimolar ratio (Fig. 3 A) and, in comparison, of a binary mixture (32 mol% DMPE<sub>d54</sub>) of ReLPS and DMPE<sub>d54</sub> (Fig. 3 B). The two synthetic phospholipids undergo the  $L_\beta \leftrightarrow L_\alpha$  phase transition at nearly identical temperatures (36°C), whereas the phase transition temperatures of pure DMPC and DMPE<sub>d54</sub> membranes are known to be at 23.6°C and at 46.2°C, respectively (Casal and Mantsch, 1984). Characteristically, the transition width of the phase transitions of each lipid component is about twofold larger for ReLPS/DMPE<sub>d54</sub> mixtures (Fig. 3 B) than for DMPC/DMPE<sub>d54</sub> mixtures (Fig. 3 A). Furthermore, the curves of the ReLPS/DMPE<sub>d54</sub> mixture show evidence of additional transition features, whereas the respective transition curves of the binary phospholipid mixture suggest the presence of a pure, ideally mixed lipid phase.

For all binary mixtures tested, the  $\theta(T)$  profiles were calculated according to procedures described in the Appendix. Table 1 summarizes the results obtained from the evaluation of the  $\tilde{\nu}_{\text{sy}}(>\text{CH}_2)$  and  $\tilde{\nu}_{\text{sy}}(>\text{CD}_2)$  marker bands, which make it possible to monitor separately the phase behavior of the ReLPS and the DMPE<sub>d54</sub>-lipid components in mixture.  $T_m$ ,  $\Delta T_m$ , and the molar fractions  $M_A$  and  $M_B$  were determined as illustrated in the Appendix (the index A is used for the pure lipid domains; B is used for the third type of domain).

As demonstrated in Table 1, the ReLPS component in mixture undergoes a phase transition around  $\sim 26^\circ\text{C}$  ( $T_{m,A}$ , A domains of ReLPS), a value close to that observed for the pure ReLPS membranes. Furthermore, fractions of the DMPE<sub>d54</sub> component exhibit a phase transition near 43°C ( $T_{m,A}$ , A domains of DMPE<sub>d54</sub>), a value also quite similar to that observed for the pure DMPE<sub>d54</sub> membranes. This indicates that pure ReLPS is present in one type of domain with a  $T_m$  at  $\sim 26^\circ\text{C}$ , and pure DMPE<sub>d54</sub> is present in a second

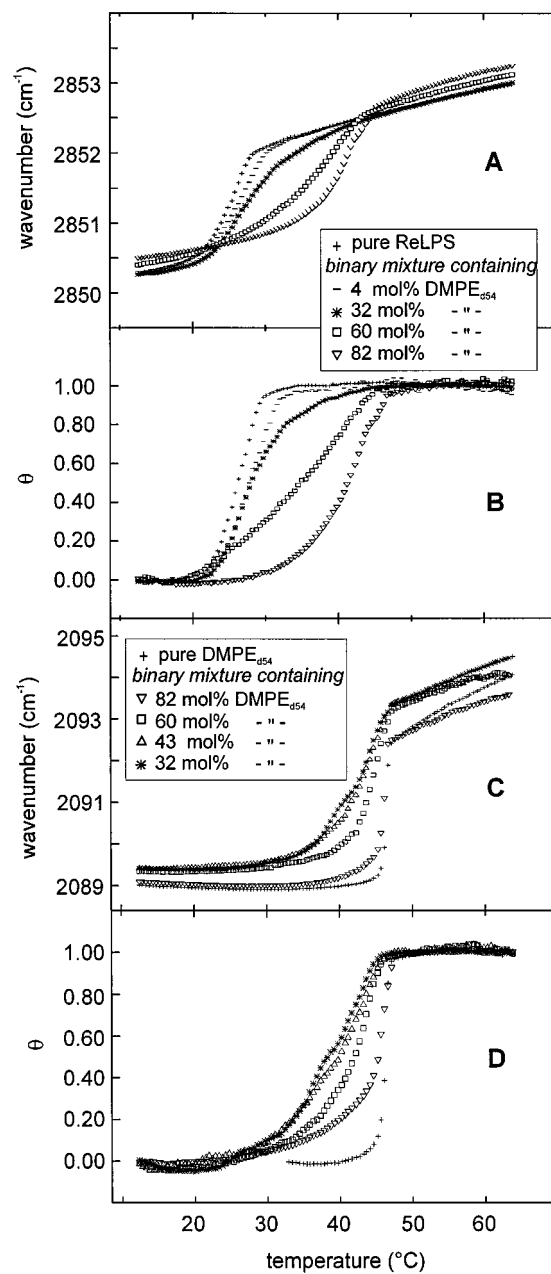


FIGURE 2 Typical temperature-induced frequency versus temperature (A and C) and fraction of melted lipids  $\theta$  versus temperature (B and D) transition profiles obtained for different binary mixtures of ReLPS  $>\text{CH}_2$ ; A and B (or  $>\text{CD}_2$ ; C and D) and DMPE<sub>d54</sub>, using the symmetrical methylene stretching band as a monitor. The composition of the mixtures varied, as indicated by the inset. The  $\theta(T)$  profile of pure DMPE<sub>d54</sub> in D was calculated for the phase transition region only.

type of domain melting between 43°C and 44°C. Between 32°C and 37°C, ReLPS and DMPE<sub>d54</sub> apparently undergo additional concomitant phase transitions ( $T_{m,B}$ , B domains of ReLPS and DMPE<sub>d54</sub>). The interpretation of this third, “domain-like” structure is more complicated and requires a model. A discussion of this phenomenon must include the following two most probable scenarios: the existence of “mixed domains” or the presence of “large interacting

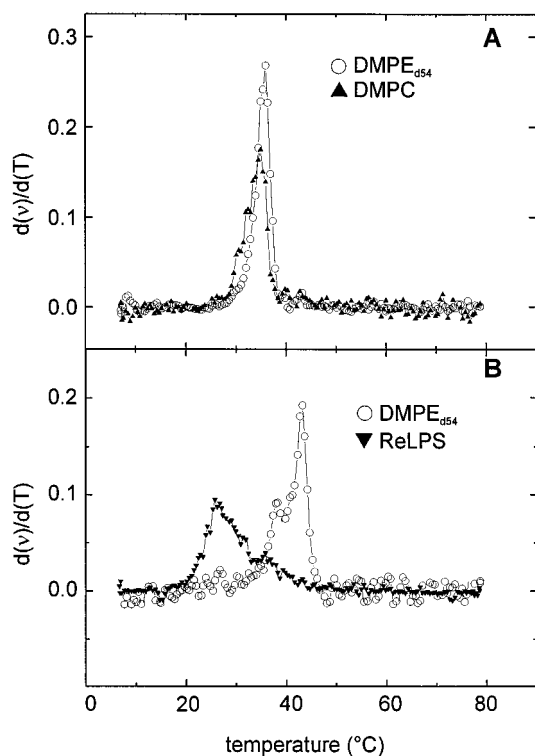


FIGURE 3 First derivatives of frequency versus temperature profiles obtained from binary mixtures of DMPC and DMPE<sub>d54</sub> in an equimolar ratio (A), and of ReLPS with DMPE<sub>d54</sub> in a molar ratio of 32:68 (B). (A) A typical example of complete miscibility leading to a single, homogeneously mixed phase. (B) The thermotropic phase behavior of a binary mixture for which the two components are segregated into domains. The phase transition temperatures of the pure components are  $T_m(\text{DMPC}) = 23.6^\circ\text{C}$ ,  $T_m(\text{DMPE}_{d54}) = 46.2^\circ\text{C}$ , and  $T_m(\text{ReLPS}) = 26.1^\circ\text{C}$ .

domain borders." This problem is further detailed in the Discussion.

From the individual fractions  $M_A$  and  $M_B$  of ReLPS summarized in Table 1, it is also evident that a higher relative amount of DMPE<sub>d54</sub> leads to a decreased amount of ReLPS present in pure domains. Remarkably, above a molar content of 60% DMPE<sub>d54</sub>, clear evidence for the presence of pure ReLPS domains can no longer be found. Similar results were obtained from the  $\theta(T)$  profiles of the DMPE<sub>d54</sub> component (see Table 1), which exhibited two separate  $T_m$  values for DMPE<sub>d54</sub>, one transition typical for domains of the pure lipid ( $T_m$  values at about  $43^\circ\text{C}$ ), and another type of domain with  $T_m$  values between  $34^\circ\text{C}$  and  $37^\circ\text{C}$ . In analogy to the results obtained for ReLPS, pure DMPE<sub>d54</sub> domains could not be observed below a DMPE<sub>d54</sub> content of  $\sim 30\%$ .

The  $T_m$ /molar fraction relationship, summarized in Table 1, is graphically illustrated by Fig. 4. From this diagram it becomes evident that at molar ratios of ReLPS/DMPE<sub>d54</sub> ranging from 70/30 to 40/60, both components (ReLPS and DMPE<sub>d54</sub>) give  $T_{m,A}$  values very close to that of the pure lipids (domains A). Furthermore, it is evident that the B-type domains of both lipids melt at significantly higher (ReLPS) or lower (DMPE<sub>d54</sub>) transition temperatures  $T_{m,B}$  than the pure lipids.

### Interaction between the polycationic polypeptide poly-(L-lysine) and the binary lipid mixtures

Poly-(L-lysine) (PLL), a polycationic polypeptide, is known to induce *in vivo* increased permeability rates of the OM toward a series of important hydrophobic drugs (Vaara and Vaara, 1983a). It has been speculated that PLL can interact with the negatively charged LPS and thereby induces the formation of pure phospholipid bilayer regions in the OM (Vaara and Vaara, 1983b). These PL bilayer domains are thought to be those regions where lipophiles may diffuse through the OM barrier. To test this assumption, high-molecular PLL<sub>(500)</sub> was added to binary lipid mixtures containing DMPE<sub>d54</sub> and ReLPS in nearly equimolar ratios. The phase behavior of the ternary system was analyzed subsequently by FTIR. The molar ratio ReLPS/PLL<sub>(500)</sub> was  $\sim 1000$ , and consequently the relation between the negatively charges of ReLPS to the positive charges of PLL<sub>(500)</sub> was adjusted to a value near 8 (at pD values near 7.2, PLL<sub>(500)</sub> has 500 positive charges and ReLPS four effective negative charges per molecule at most; Nikaido and Vaara, 1985). Fig. 5 shows typical experimental transition profiles for the untreated and the PLL<sub>(500)</sub>-treated binary mixtures. Characteristic phase transitions were observed for the ReLPS (Fig. 5 A) and the DMPE<sub>d54</sub> (Fig. 5 B) components, respectively. From the evaluation of the  $\theta(T)$  curves of the ReLPS component,  $T_{m,A}$  and  $T_{m,B}$  values were obtained at  $26.6^\circ\text{C}$  and  $35.1^\circ\text{C}$ , and from the  $\theta(T)$  profiles of the DMPE<sub>d54</sub> component, values were obtained at  $44.4^\circ\text{C}$  and  $34.7^\circ\text{C}$ , respectively (see Table 1). In comparison to the  $\theta(T)$  profiles of the binary mixtures (with comparable DMPE<sub>d54</sub>/ReLPS ratio), the PLL<sub>(500)</sub>-treated binary mixtures exhibited higher  $M_A$  and, consequently, lower  $M_B$  values for the ReLPS and DMPE<sub>d54</sub> components. Moreover, the slope (cooperativity) of the two A transitions at  $26.6^\circ\text{C}$  (pure ReLPS domains) and at  $44.4^\circ\text{C}$  (pure DMPE<sub>d54</sub> domains) was found to be close to values typical for the respective pure lipids (cf. Table 1).

### Ternary membrane systems, composed of ReLPS, DMPE<sub>d54</sub>, and porin (OmpF)

To study the interaction of the outer membrane protein OmpF with ReLPS and to test the domain structure in the presence of this most common intrinsic outer membrane protein, OmpF was integrated in binary mixtures of ReLPS and DMPE<sub>d54</sub>. These ternary membranes were subsequently investigated by FTIR spectroscopy. The addition of DMPE<sub>d54</sub> was essential, because it is known that the presence of phospholipids significantly promotes the integration of porin into lipid bilayer structures (Wiese et al., 1994). Per 1 mg ReLPS we have integrated 0.50, 0.38, and 0.25 mg OmpF to yield molar ratios of LPS/OmpF of  $\sim 14$ ,  $\sim 18$ , and  $\sim 24$ , respectively, whereas the ReLPS/DMPE<sub>d54</sub> ratio was adjusted to be  $\sim 39\%$  for all three preparations (Table 1). Usually isolated OmpF is stabilized by detergents (e.g., by o-POE) to prevent the protein from self-aggregation. How-

**TABLE 1** Phase transition parameters obtained for the binary lipid mixtures composed of ReLPS and DMPE<sub>d54</sub>, the binary mixtures interacting with PLL<sub>(500)</sub>, and the ternary system ReLPS/DMPE<sub>d54</sub>/OmpF

Composition of the mixtures*	[°C] $T_{m,A}^{\#§}$	[kJ/mol] $\Delta H_{m,A}^{\ddagger}$	$M_A$	[°C] $T_{m,B}^{\#}$	$M_B$
ReLPS-component ( $\tilde{\nu}_{sy}(>CH_2)$ modes)					
ReLPS (pure membrane)	26.1	467	1.00	—	—
32% DMPE <sub>d54</sub>	26.6	557	0.55	32.4	0.45
43% DMPE <sub>d54</sub>	27.1	336	0.33	36.5	0.67
60% DMPE <sub>d54</sub>	25.9	395	0.22	37.3	0.78
46% DMPE <sub>d54</sub> + PLL <sub>(500)</sub> , (10 <sup>3</sup> LPS/PLL)	26.6	469	0.57	35.1	0.43
47% DMPE <sub>d54</sub> + OmpF, (14:1 LPS/OmpF)	42.3	590	0.74	34.0	0.26
38% DMPE <sub>d54</sub> + OmpF, (18:1 LPS/OmpF)	42.5	646	0.63	35.4	0.37
30% DMPE <sub>d54</sub> + OmpF, (24:1 LPS/OmpF)	42.1	578	0.45	35.4	0.55
DMPE <sub>d54</sub> -component ( $\tilde{\nu}_{sy}(>CD_2)$ modes)					
32% DMPE <sub>d54</sub>	43.0	932	0.23	36.0	0.77
43% DMPE <sub>d54</sub>	43.3	832	0.44	35.5	0.56
60% DMPE <sub>d54</sub>	43.5	935	0.64	35.6	0.36
DMPE <sub>d54</sub> (pure membrane)	46.2	1694	1	—	—
46% DMPE <sub>d54</sub> + PLL <sub>(500)</sub> , (10 <sup>3</sup> LPS/PLL)	44.4	846	0.71	34.7	0.29
47% DMPE <sub>d54</sub> + OmpF, (14:1 LPS/OmpF)	42.4	622	0.54	33.4	0.46
38% DMPE <sub>d54</sub> + OmpF, (18:1 LPS/OmpF)	42.3	582	0.54	33.9	0.46
30% DMPE <sub>d54</sub> + OmpF, (24:1 LPS/OmpF)	41.9	532	0.46	32.2	0.55

\*Estimated errors in lipid composition:  $\pm 3\%$ .

#The index A is used to mark phase transition parameters of the core domains of the pure lipid components; index B is used to mark the third domain type.

§Estimated errors for  $T_m$  values:  $\pm 0.3^\circ\text{C}$ .

‡Estimated errors in kJ/mol for  $\Delta H_m$ :  $\pm 20\%$ .

ever, detergents themselves are membrane-active compounds and strongly influence the state of order of any lipid membrane. FTIR spectroscopic investigations on a ternary system in the presence of o-POE exhibited coinciding phase transition temperatures at  $\sim 21^\circ\text{C}$  for the ReLPS and DMPE<sub>d54</sub> components (data not shown). In these cases, the respective van't Hoff enthalpies  $\Delta H_m$  indicated significantly decreased and nearly identical values. Thus, to study the influence of OmpF on binary mixtures of ReLPS and DMPE<sub>d54</sub>, the detergent had to be removed quantitatively by extensive dialysis after integration of OmpF into the mixed membranes. Because the pure detergent gives rise to

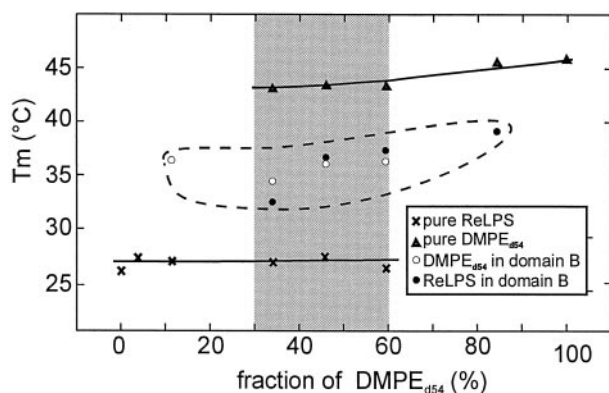


**FIGURE 4** A graphical illustration of the  $T_m$  values of ReLPS/DMPE<sub>d54</sub> mixtures differing in lipid composition. At least for binary mixtures containing 30–60% DMPE<sub>d54</sub>, pure domains of ReLPS and DMPE<sub>d54</sub> are found (gray region). A third, domain-like structure is also suggested by this representation.

strong IR absorption bands at  $1349\text{ cm}^{-1}$  and  $2855\text{ cm}^{-1}$ , complete absence of these bands in the IR spectra was taken as an indication that o-POE was completely removed.

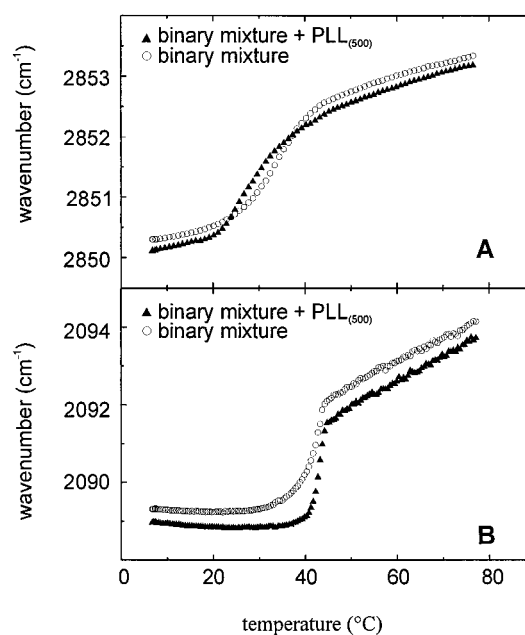


**FIGURE 5** Comparison of experimental the phase transition profiles  $\tilde{\nu}(T)$  obtained for a binary mixture of ReLPS, DMPE<sub>d54</sub>, and for a binary mixture interacting with the extrinsic, high molecular polypeptide poly-(L-lysine) (PLL<sub>(500)</sub>). In both cases the ReLPS/DMPE<sub>d54</sub> ratio was  $\sim 1:1$ . (A) The influence of PLL<sub>(500)</sub> on the ReLPS component. (B) The corresponding phase transition profiles for the DMPE<sub>d54</sub> component, using the  $\tilde{\nu}_{sy}(>CD_2)$  band as a monitor.

Again, the  $\theta(T)$  profiles of the ternary systems were calculated from the experimental band parameters of the  $>\text{CH}_2$  and  $>\text{CD}_2$  symmetrical stretching bands. Some of the experimental data (frequency versus temperature profiles) are given in Fig. 6, A and B, respectively. As expected, OmpF preferentially interacted with the naturally occurring lipid component ReLPS, and as for the binary mixtures, the  $\theta(T)$  profiles could be satisfactorily fitted by two fit functions (see Appendix). In this way,  $T_m$  values were obtained for the ReLPS component at  $\sim 42^\circ\text{C}$  and  $\sim 35^\circ\text{C}$ , respectively. For further data interpretation, it was essential to know which of the  $T_{m,A}$  or  $T_{m,B}$  values can be assigned to the ReLPS fraction that interacts directly with OmpF. Details of this assignment problem are given in the Discussion. In contrast to the ReLPS component, the two transition temperatures  $T_{m,A}$  and  $T_{m,B}$  of the  $\text{DMPE}_{d54}$  component were found to be nearly unchanged with values at  $\sim 42^\circ\text{C}$  and  $\sim 34^\circ\text{C}$  for the binary and ternary mixtures, respectively.

## DISCUSSION

The results obtained for the binary and ternary mixtures of ReLPS,  $\text{DMPE}_{d54}$ ,  $\text{PLL}_{(500)}$ , and OmpF demonstrate the potential of FTIR spectroscopy for the analysis of lipid miscibility, domain structure, and cation- or protein-induced lateral phase separation phenomena (cf. also Dluhy et al., 1983). The use of lipid mixtures in which one of the lipid components has perdeuterated acyl chains provides the clear advantage of being able to monitor the order parameters of each lipid component in the mixture simultaneously in a

single experiment without the use of any perturbing probe molecules.

## Binary lipid mixtures

The temperature-induced phase transition profiles detected for the two components ReLPS and  $\text{DMPE}_{d54}$  provide ample evidence that pure domains of ReLPS and  $\text{DMPE}_{d54}$  coexist at least in mixtures containing  $\text{DMPE}_{d54}$  in molar fractions ranging from 30% to 60% (see *gray region* in Fig. 4). However, as suggested by Table 1, considerable amounts of the two lipid components definitely melt at temperatures distinctly different from the melting points of corresponding pure substances. One may then ask questions about the structure or the molecular organization of this third type of "domain." First, the correspondence of the  $T_{m,B}$  values obtained for ReLPS and  $\text{DMPE}_{d54}$  may simply suggest the presence of mixed domains. However, a different interpretation model may be particularly valid. For an understanding of the molecular organization of these "B domains," it must be pointed out that the real shapes of the  $\theta(T)$  transition profiles strongly give rise to the supposition that this third type of "domain-like" structure is not as homogeneous as suggested by the nearly coinciding  $T_{m,B}$  values. It seems rather more likely that these "domains" are defined by a situation in which the pure lipid domains are surrounded by several two-dimensional layers of lipid molecules. As a consequence, the pure domains are either stabilized (ReLPS) or disturbed ( $\text{DMPE}_{d54}$ ) by their specific environments, represented by the adjacent  $\text{DMPE}_{d54}$  and ReLPS molecules, respectively. In other words, it is more plausible to presume that binary mixtures of lipids—being as different as ReLPS and  $\text{DMPE}_{d54}$ —are not miscible at all, but will rather tend to assemble in small domains of the pure lipid components, which at their border regions are mutually influenced by the adjacent molecules of the neighboring domains. One consequence of this model would be that with increasing distance from the domain borders, the state of order becomes more similar to that of a pure lipid component. In Fig. 7 we have tried to make the latter considerations intelligible. This figure shows a typical  $\theta(T)$  phase transition profile obtained for the  $\text{DMPE}_{d54}$  component in a binary mixture. The relative amount of  $\text{DMPE}_{d54}$  molecules in pure domains ("A domain") and the contribution from  $\text{DMPE}_{d54}$  molecules residing in two-dimensional layers at the domain borders ("B domain") give rise to the particular shape of the phase transition profiles. From Fig. 7 it also becomes evident that the  $\Delta H_{m,B}$  values have no clear physical significance, because the phase behavior of the B domains is quite heterogeneous.

Another aspect concerns the fact that pure domains of ReLPS and  $\text{DMPE}_{d54}$  are found for most of the binary mixtures. If ReLPS and  $\text{DMPE}_{d54}$  were really miscible, one would expect for a binary mixture either one single mixed phase (if the lipids are miscible in any ratio) or (if ReLPS and  $\text{DMPE}_{d54}$  are only partially miscible) one pure A com-

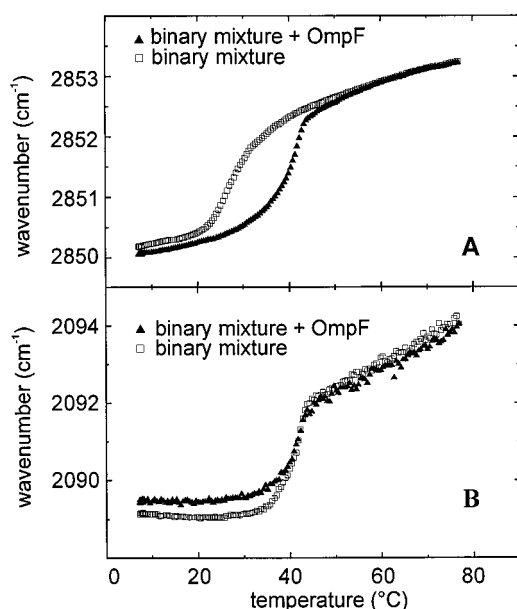


FIGURE 6 Comparison of the phase transition profiles  $\tilde{\nu}(T)$  obtained for a ternary mixture of ReLPS,  $\text{DMPE}_{d54}$ , and OmpF and a binary mixture of ReLPS and  $\text{DMPE}_{d54}$ . The ReLPS/ $\text{DMPE}_{d54}$  ratio was in both cases  $\sim 1:1$ . (A) The influence of OmpF on the ReLPS component, using the  $\tilde{\nu}_{\text{sy}}(>\text{CH}_2)$  band as a monitor. (B) The corresponding phase transition profiles, which illustrate the influence of OmpF on the  $\text{DMPE}_{d54}$  component.

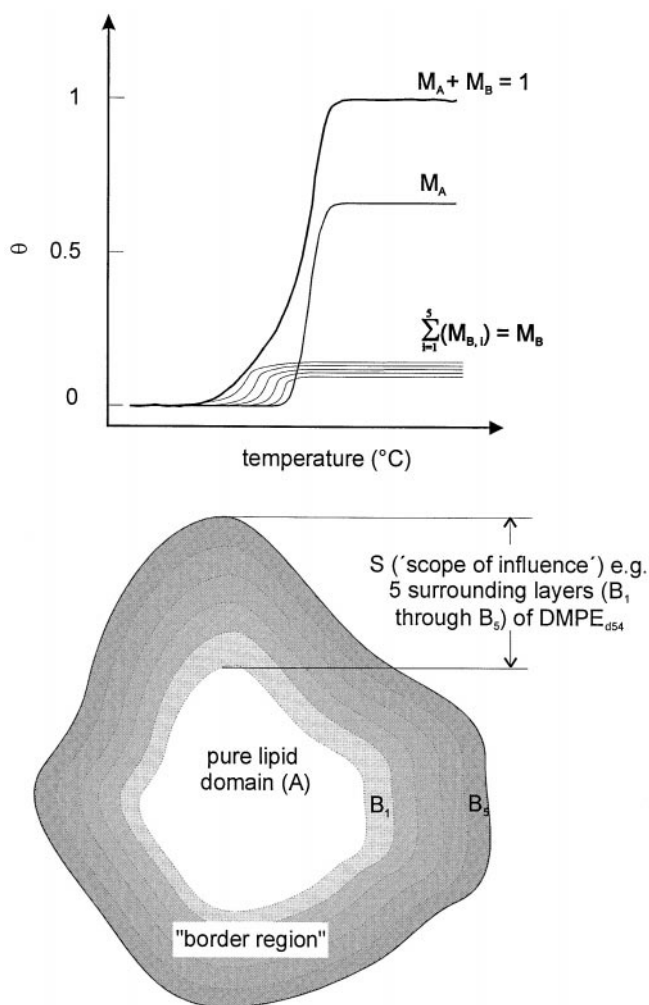


FIGURE 7 Illustration of how the shape of the  $\theta(T)$  transition profiles can be explained by the “border model,” using the example of a  $\theta(T)$  profile of the DMPE<sub>d54</sub> component of a binary mixture of ReLPS and DMPE<sub>d54</sub>. It is assumed that a “core domain” of the pure DMPE<sub>d54</sub> is surrounded by various layers of DMPE<sub>d54</sub> molecules, constituting a so-called scope of influence,  $S$ . These layers are influenced by the second component, in this case by ReLPS. The experimental transition profile can thus be thought to be the superposition of the transition of the pure domain A and the individual transitions of the different layers surrounding domain A (in this case, five layers,  $B_1$  through  $B_5$ ,  $\sum M_{B,i} = M_B$ ).

ponent (either ReLPS or DMPE<sub>d54</sub>) and one single type of mixed domains. Consequently, the presence of two different types of pure domains is explained most reasonably by the proposed border model, although the mixed domain model cannot be ruled out completely.

If one accepts that the border model is valid, the relatively large  $M_B$  values found for all mixtures can be taken as an indication of the prevalence of relatively small domains. Then it is possible to estimate the absolute size of the pure domains. For this purpose it is necessary to estimate the so-called scope of influence  $S$ , i.e., the distance from the domain border to a region where the state of order is expected to be unchanged and equals the pure component (see Fig. 7 and Appendix). If one assumes that the domains can be

approximated by circular areas, one can estimate the diameter of the unperturbed pure domain (the A domains) by simple geometrical considerations (see Appendix), provided that the value of the  $S$  is known. By Langmuir-Blodgett measurements, area values per fatty acid chain of the used ReLPS charge have been determined to be comparable to that obtained for typical phospholipids ( $\sim 0.2 \text{ nm}^2$ ) (Schultz, 1993). These observations were found to be in accordance to data of x-ray studies (Labischinski et al., 1985,  $\sim 0.181 \text{ nm}^2$ ; Kato et al., 1990,  $\sim 0.185 \text{ nm}^2$ ) and molecular modeling calculations (Kastowsky et al., 1991). Furthermore, it is known that ReLPS molecules have six (hexaacyl form) or seven (heptaacyl form) and DMPE<sub>d54</sub> two fatty acids per residue. If one assumes, for example, that  $S = 5$  (as depicted in Fig. 7) layers of DMPE<sub>d54</sub>, one can calculate for the pure, unperturbed domains diameters of  $r_A \approx 3.5 \text{ nm}$  for a 32 mol% DMPE<sub>d54</sub> mixture and  $r_A \approx 7 \text{ nm}$  for a mixture with 43 mol% DMPE<sub>d54</sub> (for calculation of  $r_A$  values, see Appendix). Table 2 gives an overview of these  $r_A$  values. The diameters  $r_A$  were estimated assuming a thickness of five or three layers of ReLPS and DMPE<sub>d54</sub> molecules, respectively, as the arbitrary value of  $S$ . Thus, although these calculations can be taken only as rough approximations from a theoretical point of view, the method turns out to be quite useful for comparative analysis in practice.

### Interaction of binary mixtures with the extrinsic protein poly-(L-lysine)

The polycationic polypeptide poly-(L-lysine) (PLL<sub>(500)</sub>) interacts with the negatively charged ReLPS molecules and affects the thermotropic phase behavior of the deuterated phospholipid DMPE<sub>d54</sub>. This fact is evident from the shape of the phase transition profiles. Whereas the phase transition temperatures are virtually unchanged by PLL<sub>(500)</sub>, the  $M_A$  and  $M_B$  values undergo significant changes. In comparison to the phase transition profiles of the binary mixtures, the  $M_A$  values of the PLL<sub>(500)</sub>-treated mixtures (i.e., the part of lipids coexisting in “pure domains”) are increased for both amphiphiles, which, in accordance with the border model, lends strong support to the supposition that PLL<sub>(500)</sub> is able to induce increased domain sizes. Calculations on the basis

TABLE 2 Estimated radii of pure lipid domains as calculated from the  $M_A$  and  $M_B$  values

Composition of the binary mixtures	Domain radius (nm)	
	ReLPS-domains*#	DMPE <sub>d54</sub> -domains*#
32% DMPE <sub>d54</sub>	17 (10)	3.5 (2)
43% DMPE <sub>d54</sub>	7 (5)	7 (4)
60% DMPE <sub>d54</sub>	5 (3)	15 (9)
46% DMPE <sub>d54</sub> + PLL <sub>(500)</sub> (10 <sup>3</sup> LPS/PLL)	18 (11)	20 (12)
38% DMPE <sub>d54</sub> + OmpF, (18:1 LPS/OmpF)	22 (13)	10 (6)

\*Estimated errors:  $\pm 50\%$ .

#The radii were calculated assuming values of  $S$  (scope of influence) of five and three (in parentheses) surrounding layers of lipids.



of the above-mentioned model yielded radii of  $\sim 18$  or  $\sim 11$  nm for ReLPS and  $\sim 20$  or  $\sim 12$  nm for the DMPE<sub>d54</sub> component, assuming reasonable values of five or three lipid layers, respectively, for *S*. Consequently, the domain area was increased by more than fourfold after the addition of PLL<sub>(500)</sub>. Thus, although the model used for data interpretation requires a couple of assumptions and idealizations, the induction of larger domain sizes due to the interaction of PLL<sub>(500)</sub> with the ReLPS component of the binary mixture is, at least in a semiquantitative sense, out of the question. PLL<sub>(500)</sub> induces no major  $T_m$  shifts for the DMPE<sub>d54</sub> or the ReLPS components for the given concentrations. The apparent  $T_m$  shifts suggested by Fig. 5 can be sufficiently explained by the proposed border model as the effect of mutually changed  $M_A$  and  $M_B$  values. It may be that PLL<sub>(500)</sub> is able to link up the charged ReLPS headgroups via electrostatic interactions, thus inducing increased ReLPS and, as a secondary effect, increased DMPE<sub>d54</sub> domain sizes. This type of interaction is therefore assumed to induce primarily headgroup-mediated domain reorganization, a statement that contrasts with the effects of the intrinsic membrane protein OmpF.

### Interaction of binary lipid mixtures with the intrinsic protein OmpF

The main conclusion that can be drawn from the results of Fig. 6 is the following. The integral outer membrane protein OmpF interacts preferentially with the ReLPS component in mixed membranes. Apparently OmpF causes a significant upshift of  $T_m$  and an increased state of order of the ReLPS component, indicating strong stabilizing effects exerted by the protein. In contrast, the interactions of porin with the DMPE<sub>d54</sub> component are weak but characteristic for non-specific interactions between a typical phospholipid and a membrane protein. The state of order of DMPE<sub>d54</sub> is only slightly decreased before and very slightly increased after the phase transition, whereas the cooperativity of the transition is reduced. The latter findings are in good agreement with literature data describing nonspecific lipid/protein interactions (Curatolow et al., 1977; Chapman et al., 1979; Gomez-Fernandez et al., 1980; Heyn et al., 1981).

For a detailed characterization of the molecular interactions between ReLPS and OmpF, it is important to know which ReLPS subpopulation (A, with a  $T_{m,A}$  of  $\sim 42^\circ\text{C}$ , or B, with a  $T_{m,B}$  of  $34^\circ\text{C}$ ) has direct contact sites with the OmpF trimers. Starting with the assumption that at different LPS/OmpF molar ratios (but always ratios with an excess of lipopolysaccharide), the number of LPS molecules in the direct vicinity of OmpF should be roughly constant, we could assign the A domains of ReLPS as the ReLPS subpopulations that strongly and directly interact with OmpF. This assumption is backed by two facts. First, phase transition temperatures near  $42^\circ\text{C}$  have never been obtained for ReLPS in the absence of OmpF, for pure ReLPS or for ReLPS/DMPE binary lipid mixtures. Second, we found that

with increasing ReLPS/OmpF ratios, the  $M_A$  values were decreased. Calculations based on different ReLPS/OmpF ratios and the  $M_A$  values proved the constancy of the number of ReLPS molecules that are in direct contact with the OmpF trimer (i.e., 10–12 LPS per OmpF) for all three ternary membrane preparations tested (see Table 1). The characterization of the second LPS subpopulation (B domain), which gives  $T_m$  values between  $34^\circ\text{C}$  and  $36^\circ\text{C}$ , is much more complicated, because the effects of ReLPS-DMPE<sub>d54</sub> and ReLPS-ReLPS/OmpF interactions are superimposed. As already mentioned, the FTIR spectroscopic characterization of membranes composed only of ReLPS and OmpF is hindered by the fact that the integration of OmpF into LPS membranes is much more effective if phospholipids are present (Wiese et al., 1994). It is particularly interesting that the ReLPS molecules that interact with the porin gave rise to a very pronounced and even sharper phase transition profile than that observed for the OmpF-free binary mixtures (the  $T_{m,A}$  value is increased by  $\sim 17$  K!). This fact, the particularly high cooperativity of the  $T_{m,A}$  transition, characterizes a surprising and, to the knowledge of the authors, hitherto undescribed type of lipid/protein interaction. Most of the authors, who investigated mixed systems of membrane proteins and synthetic phospholipids, stated that membrane proteins lower the phase transition temperature and lower the  $\Delta H_m$  values of the surrounding lipid layer. Obviously, OmpF may exert a very specific effect on the ReLPS component.

The simple calculations based on the border model (see Fig. 7 and the Appendix) suggested that every OmpF trimer interacts directly with  $\sim 10$ – $12$  ReLPS molecules. This number of ReLPS molecules per porin seems to be realistic. Simple geometrical considerations based on Langmuir-Blodgett or x-ray diffraction data for ReLPS (Kato et al., 1990; Schultz, 1993) and x-ray diffraction data of OmpF (Cowan et al., 1992) suggest that  $\sim 30$  ReLPS molecules can reside in the immediate vicinity of one porin trimer, provided that both the “extracellular” and the “periplasmic” halves of OmpF are exposed to ReLPS. In vivo this number should be decreased to less than 15, because the OM is a highly asymmetrical membrane containing LPS only in its extracellular leaflet. Our findings suggest that 10–12 ReLPS molecules are located next to OmpF, which is quite close to the number 15. This fact and the observation that different types of lipid-protein interactions are present in one and the same lipid mixture may give rise to speculations that OmpF has induced the segregation of asymmetrical lipid clusters in mixed vesicles. This notion, i.e., one LPS solvation layer surrounding every trimer preferentially at the extracellular part of OmpF, and a phospholipid environment (DMPE) at the periplasmic porin surface, may be taken as one explanation of our experimental results. Thus strong LPS-OmpF interactions on the extracellular part of OmpF, together with highly specific binding sites for LPS, could be the driving force for the appearance of asymmetry in such bilayers in vivo and may further explain the appearance of PL in the outer leaflet of the OM in LPS-defect

mutants that are known to express reduced amounts of porin (Ames et al., 1974; Nikaido and Vaara, 1985). The molecular nature of the LPS/OmpF interactions, however, still has to be described in detail. Particular candidates for specific LPS/OmpF interactions are the hydroxyl groups of the  $\beta$ -hydroxy fatty acids and the  $>C=O$  carbonyls of the ester and amide bound fatty acids of the lipid A anchor of LPS. Future FTIR experiments on the LPS/PL/OmpF mixture, using  $^{13}C=O$ -labeled DMPE to spectroscopically separate the various  $>C=O$  carbonyl functions of LPS and PL, are necessary to scrutinize these assumptions.

Porin/DMPE interactions are of the pure hydrophobic type, and are most probably mediated by the acyl chains of the phospholipid and the hydrophobic amino acid side chains at the boundary surface of OmpF (Cowan et al., 1992). Whereas the induction by OmpF of asymmetrical lipid clusters in its immediate vicinity is only one (but the most plausible) of several scenarios, the existence of different lipid domains in ternary membranes of ReLPS, DMPE<sub>d54</sub>, and OmpF is beyond question. Applying the described border model and comparing the resulting domain sizes with data calculated for the ternary and the binary mixtures (cf. Table 2), one can easily see that in ternary mixtures, domains containing ReLPS are generally increased in size. This fact indicates again the preference of OmpF-ReLPS interactions in the ternary system. These considerations are in good accordance with literature data on other membrane proteins, such as protein A (Haverstick and Glaser, 1989), lipophilin (Boggs et al., 1977), and D- $\beta$ -hydroxybutyrate dehydrogenase (Wang et al., 1988), illustrating that integral membrane proteins may interact preferentially with one type of phospholipid and build up a nonrandom distribution of lipids in their immediate vicinity.

The findings of stable pure domains made up by DMPE<sub>d54</sub> in binary and ternary structures are consistent with results published by the group of Nikaido (see, e.g., Takeuchi and Nikaido, 1981), which already stated, on the basis of electron spin resonance measurements on LPS/PE mixtures, that LPS and PE are segregated in separate lipid domains. This may suggest that similar PL domains are also present in vivo, i.e., in the outer OM leaflet of Gram-negative bacteria exhibiting defective LPS structures (Nikaido and Vaara, 1985). In fact, such symmetrical phospholipid bilayer domains are the only loci where hydrophobic molecules like hydrophobic antibiotics may effectively penetrate the bacterial OM. Recently, Raetz and co-workers could show that an antibacterial drug (L-161, 240), a LPS biosynthesis inhibitor, had considerable in vitro activity, even against wild-type strains of *Escherichia coli*, whereas mutants with a defective outer membrane barrier function showed a minimal inhibitory concentration  $\sim 100$  times as low as for the wild-type strains of *E. coli* and other enterobacteria (Onishi et al., 1996; Vaara, 1996). In this context our findings may contribute to a better understanding of those processes controlling the self-promoted permeation of LPS biosynthesis inhibitors through the outer membrane.

## APPENDIX

### Description of the model used to generate $\theta(T)$ phase transition profiles

Fig. 8 A gives an example of frequency/temperature, intensity/temperature, and half-width/temperature profiles experimentally determined from a pure ReLPS preparation. One can easily see that the various parameter/temperature functions differ substantially and may yield quite different transition midpoint values ( $T_m$ ). It is known that two conformational populations of lipids, one characteristic of the gel and one characteristic of the liquid crystalline phase, coexist in the phase transition region. Both populations of lipids are represented in the IR spectra by typical  $\nu_{sy}(>CH_2)$  bands, which themselves are weighted by a factor  $\theta$  that quantifies the fraction of lipids in the liquid crystalline state ( $0 \leq \theta \leq 1$ ). It could be shown in the literature (Dluhy et al., 1983) that the superposition of these two bands results in nonlinear relationships between the respective band parameter and the real fraction of melted lipid  $\theta(T)$  in the phase transition region. One conclusion that can be drawn from these considerations (see also Fig. 8 A)

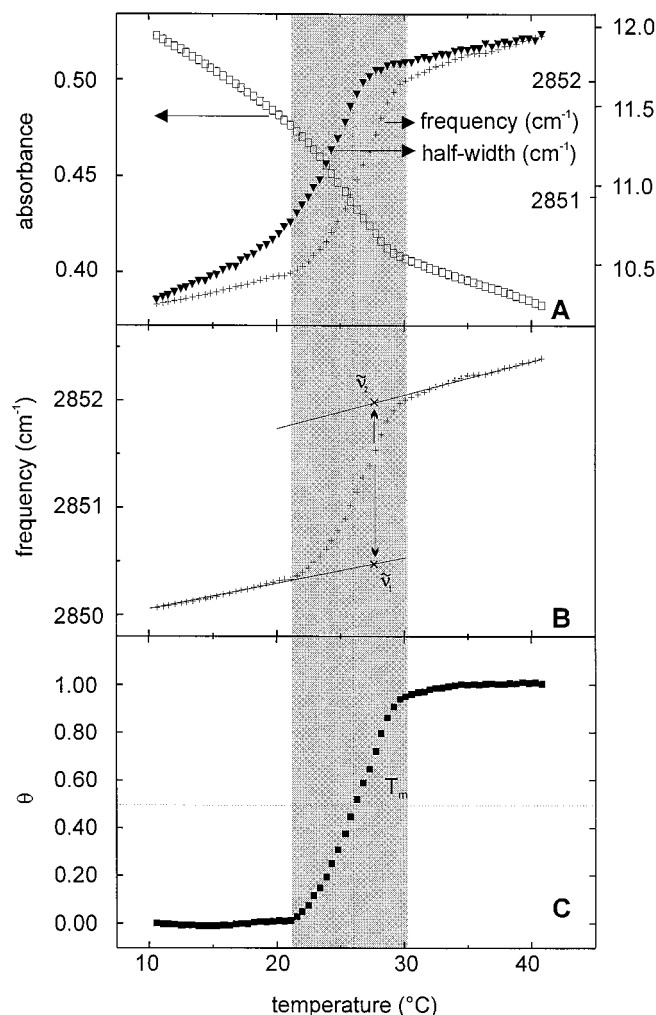


FIGURE 8 Illustration of the evaluation process used to generate  $\theta(T)$  phase transition profiles. The band parameters (frequency, bandwidth, and intensity) were first experimentally determined (A). (B) An example of how the frequency values for the gel ( $\bar{\nu}_1$ ) and liquid-crystalline ( $\bar{\nu}_2$ ) states were determined by extrapolating band parameter/temperature plots from the high- and low-temperature region through the melting interval (gray region). (C) A  $\theta(T)$  profile as calculated by formula 3 of the Appendix for a pure ReLPS preparation.

is that the discrepancy between the half-width/temperature, the frequency/temperature, and the intensity/temperature dependencies is the consequence of the overlay of the gel-state and liquid crystalline state band differing in the respective band parameters, and is not due to different physicochemical properties monitored by the half-width, frequency, or intensity parameters. Furthermore, it should be immediately evident that the larger the differences between the band parameters of the gel and liquid-crystalline state bands, the weaker the correspondence (linearity) between the frequency/temperature profiles (used in many IR studies so far published) and the phase transition  $\theta(T)$ .

Although the gel- and liquid-crystalline state bands are superimposed, it is possible to obtain the  $\theta(T)$  relationship analytically. For this purpose, a Lorentzian lineshape is assumed for the two overlapping symmetrical methylene stretching bands. The following equation describes the shape of the superimposed band at a given constant temperature (cf. Dluhy et al., 1983):

$$I(\tilde{\nu}) = (1 - \theta) \left[ \frac{I_1}{1 + 4 \left( \frac{\tilde{\nu} - \tilde{\nu}_1}{\alpha_1} \right)^2} \right] + \theta \left[ \frac{I_2}{1 + 4 \left( \frac{\tilde{\nu} - \tilde{\nu}_2}{\alpha_2} \right)^2} \right], \quad (1)$$

where  $I(\tilde{\nu})$  is the intensity as a function of frequency,  $\theta$  the fraction of lipid in the liquid crystalline state,  $\tilde{\nu}_1$  is the frequency of the gel state band,  $\tilde{\nu}_2$  is the frequency of the liquid crystalline state band,  $\alpha_1$  is the Lorentzian half-width of the ordered lipid (gel state),  $\alpha_2$  is the half-width for the liquid crystalline state,  $I_1$  is the peak intensity (absorbance) of the gel state band, and  $I_2$  is the peak intensity of the liquid crystalline state band. From Eq. 1 it is evident that the calculation of  $\theta$  requires knowledge of the band frequencies, intensities, and half-widths. It is possible to obtain these band parameters from the experimental frequency-temperature, intensity-temperature, and half-width-temperature profiles by linear extrapolation (linear regression analysis) of the high- and low-temperature region data. Fig. 9 B shows how the frequency values  $\tilde{\nu}_1$  and  $\tilde{\nu}_2$  were extrapolated. To calculate  $\theta(T)$  analytically from the experimental data, Eq. 1 has to be transformed in the following way:

$$\text{if } \frac{d[I(\tilde{\nu})]}{d(\tilde{\nu})} = 0 \quad (2)$$

then

$$\theta(T) = \frac{1}{1 - \frac{I_2(T) \cdot B(T) \cdot \alpha_1(T) \cdot (1 + 4A(T)^2)^2}{I_1(T) \cdot A(T) \cdot \alpha_2(T) \cdot (1 + 4B(T)^2)^2}} \quad (3)$$

with

$$A(T) = \frac{\tilde{\nu}(T) - \tilde{\nu}_1(T)}{\alpha_1(T)}, \quad \text{and} \quad B(T) = \frac{\tilde{\nu}(T) - \tilde{\nu}_2(T)}{\alpha_2(T)}.$$

$\tilde{\nu}(T)$  is now the frequency value at the band maximum, which can be derived easily from the experimental data for different temperatures. Equation 3 describes the functional dependency of  $\theta$  on the temperature  $T$  and the seven band parameters ( $I_1$ ,  $I_2$ ,  $\alpha_1$ ,  $\alpha_2$ ,  $\tilde{\nu}_1$ ,  $\tilde{\nu}_2$ , and  $\tilde{\nu}$ ). Fig. 9 C shows the example of a  $\theta(T)$  profile as calculated from experimental data obtained from a pure ReLPS preparation.

In the present study the thermodynamic parameters  $T_m$ ,  $\Delta H$ , and the  $M_i$  values were derived exclusively from these  $\theta(T)$  profiles.

### Determination of thermodynamic parameters from the $\theta(T)$ profiles

Thermodynamic parameters such as  $T_m$ ,  $\Delta H_m$  and molar fractions of lipids present in different states or domains can be derived from the melting

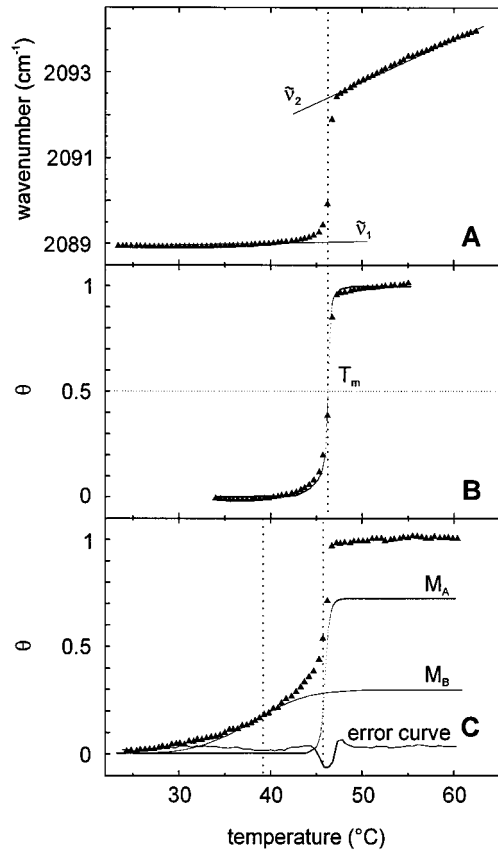


FIGURE 9 Graphical representation of an experimental  $\tilde{\nu}(T)$  profile (A) and a  $\theta(T)$  phase transition profile (B) obtained for a pure DMPE<sub>d54</sub> membrane (the profile in B was calculated for the phase transition region only). (C) The  $\theta(T)$  profile for the DMPE<sub>d54</sub> component of a typical ReLPS and DMPE<sub>d54</sub> mixture (82% DMPE<sub>d54</sub>), and an example of how the molar fractions  $M_A$  and  $M_B$  of the lipids in the domains A and B are determined from a  $\theta(T)$  profile by curve fitting.

curves  $\theta(T)$ . For this purpose, the  $\theta(T)$  profiles were first obtained according to the procedures described by Eqs. 1, 2, and 3 and then fitted using the Boltzmann function (Eq. 4), as shown for a pure DMPE<sub>d54</sub> preparation (see Fig. 9 C):

$$\theta_{(\text{FIT})}(T) = \frac{M_1 - M_2}{1 + e^{(T - T_m)/d}} + M_2, \quad (4)$$

where  $T_m$  is the phase transition temperature at  $\theta = 0.5$ ,  $M_1$  is the initial value of the transition profile ( $M_1 = 0$ ),  $M_2$  is the final value ( $M_2 = 1$ ), and  $d$  is a measure of the slope of the  $\theta(T)$  function. It is assumed that the lipids participate in a simple two-state equilibrium between the gel and the liquid-crystalline states. The van't Hoff enthalpy is then determined according to the following formula:

$$\Delta H_m = 4RT^2 \left[ \frac{d(\theta)}{d(T)} \right]_{T_m} \quad (5)$$

(Marsh et al., 1977). The slope  $[d(\theta)/d(T)]_{T_m}$  can be derived directly from Eq. 4 and was

$$\left[ \frac{d(\theta)}{d(T)} \right]_{T_m} = \frac{1}{4 \cdot d}. \quad (6)$$

In general, one particular lipid component of a given binary lipid mixture

may be present in different types of domains, e.g., in domains of the pure component and in mixed domains. Consequently, the transition function  $\theta(T)$  can be described as a sum of two (or more) independent transitions  $\theta_A$  and  $\theta_B$ :

$$\theta(T) = M_A \cdot \theta_A(T) + M_B \cdot \theta_B(T) + \dots \quad (7)$$

where  $M_A$  and  $M_B$  are the fractions of lipids, present in the domains of type A and B, and  $\theta_A$  and  $\theta_B$  are the corresponding values of the transition at particular temperatures.  $M_A$  and  $M_B$  are assumed to be independent of the temperature  $T$ . It is further assumed that in the presence of a two-domain system,  $M_A + M_B = 1$ . The  $M_A$  and  $M_B$  values were obtained from the transition profiles by curve fitting with a sum of two Boltzmann functions, as described by

$$\theta_{(\text{FIT})}(T) = M_A \cdot \left[ 1 - \frac{1}{1 + e^{(T-T_{m,A})/d_A}} \right] + M_B \cdot \left[ 1 - \frac{1}{1 + e^{(T-T_{m,B})/d_B}} \right] \quad (8)$$

This curve fitting can be carried out for both lipid components of the binary mixture, as illustrated by Fig. 9 C for DMPE<sub>d54</sub>. The knowledge of  $M_A$  and  $M_B$  from "pure" binary mixtures and binary lipid mixtures interacting with membrane-active agents makes it possible to semiquantitatively describe lateral phase separation processes.

### The estimation of the absolute domain sizes using the $M_A$ and $M_B$ values

Fig. 7 schematically illustrates the border model (see Discussion), assuming domains of the pure lipid (domain A) surrounded by several "disturbed" layers of the same lipid (domain B). If the domain shape is considered as a circular area, and if it is also assumed that the ratio of these areas  $A_A/A_B$  equals the ratio of  $M_A/M_B$ , one can yield, by simple geometrical considerations,

$$\frac{M_A}{M_B} = \left[ \frac{\pi \cdot r_A^2}{\pi \cdot (r_A + S)^2 - \pi \cdot r_A^2} \right] \quad (9)$$

where  $r_A$  is the (average) radius of the circular areas of domain A, and  $S$  is the arbitrary "scope of influence." The  $S$  values were estimated for DMPE<sub>d54</sub> and ReLPS as the distances from the respective phase borders to a region where the state of order is expected to be unchanged. With a knowledge of  $S$  and  $M_A/M_B$ , it is possible to find  $r_A$ . Table 2 gives for the DMPE<sub>d54</sub> and ReLPS components the  $r_A$  values as a function of the lipid composition and for the PLL<sub>(500)</sub>- or OmpF-treated membranes. It should be emphasized that values of  $r_A$  can only be taken as semiquantitative.

We thank Dr. H. Brade (Forschungsinstitut Borstel) for providing the samples of pure ReLPS. Particular thanks are extended to Prof. Rosenbusch and G. Rummel (Biozentrum, Basel) for the kind gifts of OmpF. We thank Mrs. A. Brauer for her excellent help in preparation of the manuscript.

This work was supported by the Deutsche Forschungsgemeinschaft (grant Na 226/1).

### REFERENCES

Ames, G. F.-L., E. N. Spudich, and H. Nikaido. 1974. Protein composition of the outer membrane of *Salmonella typhimurium*: effect of lipopolysaccharide mutations. *J. Bacteriol.* 117:406–416.

Boggs, J. M., D. D. Wood, M. A. Moscarello, and D. Papahadjopoulos. 1977. Lipid phase separation induced by a hydrophobic protein in phosphatidylserine-phosphatidylcholine vesicles. *Biochemistry.* 16: 2325–2329.

Casal, H. L., and H. H. Mantsch. 1984. Polymorphic phase behavior of phospholipid membranes studied by infrared spectroscopy. *Biochim. Biophys. Acta.* 779:381–401.

Chapman, D., J. C. Gomez-Fernandez, and F. M. Goni. 1979. Intrinsic protein lipid interactions physical and biochemical evidence. *FEBS Lett.* 98:211–223.

Cowan, S. W., T. Schirmer, G. Rummel, M. Steiert, R. Ghosh, R. A. Pauptit, J. N. Jansonius, J. P. Rosenbusch. 1992. Crystal structure explain functional properties of two *Escherichia coli* proteins. *Nature.* 358:727–733.

Curatolo, W., J. D. Sakura, D. M. Small, and G. G. Shipley. 1977. Protein lipid interactions recombinants of the proteolipid apoprotein of myelin with dimyristoyllecithin. *Biochemistry.* 16:2313–2319.

Dluhy, R. A., R. Mendelsohn, H. L. Casal, and H. H. Mantsch. 1983. Interaction of dipalmitoylphosphatidylcholine and dimyristoylphosphatidylcholine-d<sub>54</sub> mixtures with glycophorin. A Fourier transform infrared investigation. *Biochemistry.* 22:1170–1177.

Fried, V. A., and L. Rothfield. 1978. Interactions between lipopolysaccharide and phosphatidylethanolamine in molecular monolayer. *Biochim. Biophys. Acta.* 514:69–82.

Galanos, C., and O. Lüderitz. 1975. Electrodialysis of lipopolysaccharides and their conversion to uniform salt forms. *Eur. J. Biochem.* 54: 603–610.

Garavito, R. M., and J. P. Rosenbusch. 1986. Isolation and crystallization of bacterial porin. *Methods Enzymol.* 125:309–328.

Gomez-Fernandez, J. C., F. M. Goni, D. Bach, C. J. Restall, and D. Chapman. 1980. Protein lipid interaction biophysical studies of calcium magnesium ATPase EC-3.6.1.3 reconstituted systems. *Biochim. Biophys. Acta.* 598:502–516.

Haverstick, D. M., and M. Glaser. 1989. Influence of proteins on the reorganization of phospholipid bilayers into large domains. *Biophys. J.* 55:677–682.

Heyn, M. P., A. Blume, M. Rehorek, and N. A. Dencher. 1981. Calorimetric and fluorescence depolarization studies on the lipid phase transition of bacteriorhodopsin dimyristoylphosphatidylcholine vesicle. *Biochemistry.* 20:7109–7115.

Jones, N. J., and M. J. Osborn. 1977. Interaction of *Salmonella typhimurium* with phospholipid vesicles. Incorporation of exogenous lipids into intact cells. *J. Biol. Chem.* 252:7398–7404.

Kamio, Y., and H. Nikaido. 1976. Outer membrane of *Salmonella typhimurium*: accessibility of phospholipid headgroups to phospholipase C and cyanogen bromide activated dextran in the external medium. *Biochemistry.* 15:2561–2570.

Kastowsky, M., A. Sabisch, T. Gutberlet, and H. Bradaczek. 1991. Molecular modelling of bacterial deep rough mutant lipopolysaccharide of *Escherichia coli*. *Eur. J. Biochem.* 197:707–716.

Kato, N., M. Ohta, N. Kido, H. Ito, S. Naito, T. Hasegawa, T. Watabe, and K. Sasaki. 1990. Crystallization of R-form of lipopolysaccharides from *Salmonella minnesota* and *Escherichia coli*. *J. Bacteriol.* 172: 1516–1528.

Kouaoui, R., J. R. Silvius, I. Graham, and M. Pezolet. 1985. Calcium induced lateral phase separations in phosphatidylcholine-phosphatic acid mixtures. A Raman spectroscopic study. *Biochemistry.* 24:7132–7140.

Labischinski, H., G. Barnickel, H. Bradaczek, D. Naumann, E. Th. Rietschel, and P. Giesbrecht. 1985. High state of order of isolated bacterial lipopolysaccharide and its possible contribution to the permeation barrier property of the outer membrane. *J. Bacteriol.* 162:9–20.

Mabrey, S., and J. M. Sturtevant. 1976. Investigation of phase transitions of lipids and lipid mixtures by high sensitivity differential scanning calorimetry. *Proc. Natl. Acad. Sci. USA.* 73:3862–3866.

Marsh, D., A. Watts, and P. F. Knowles. 1977. Cooperativity of phase transition in single and multibilayer lipid vesicles. *Biochim. Biophys. Acta.* 465:500–514.

Marvin, H. J. P., M. B. A. Ter Beest, D. Hoekstra, and B. Withold. 1989. Fusion of small unilamellar vesicles with viable EDTA-treated *Escherichia coli* cells. *J. Bacteriol.* 171:5268–5275.

Nabedryk, E., R. M. Garavito, and J. Breton. 1988. The orientation of  $\beta$ -sheets in porin. A polarized FT-IR investigation. *Biophys. J.* 35: 671–676.

Naumann, D., C. Schultz, A. Sabisch, M. Kastowsky, and H. Labischinski. 1989. New insights into the phase behavior of a complex anionic

- amphiphile: architecture and dynamics of bacterial deep rough lipopolysaccharide membrane as seen by FT-IR, x-ray, and molecular modeling techniques. *J. Mol. Struct.* 314:213–246.
- Nikaido, H. 1979. Nonspecific transport through the outer membrane. In *Bacterial Outer Membranes*. M. Inouye, editor. John Wiley and Sons, New York. 361–407.
- Nikaido, H. 1990. Permeability of the lipid domains of bacterial membranes. In *Membrane Transport and Information Storage*. R. C. Aloia, editor. Alan R. Liss, New York. 165–190.
- Nikaido, H., and T. Vaara. 1985. Molecular basis of bacterial outer membrane permeability. *Microbiol. Rev.* 49:1–32.
- Onishi, R. H., B. A. Pelak, L. S. Gerckens, L. L. Silver, F. M. Kahan, M. H. Chen, A. A. Patchett, S. M. Galloway, S. A. Hyland, M. S. Anderson, and C. R. H. Raetz. 1996. Antibacterial agents that inhibit lipid A biosynthesis. *Science*. 274:980–982.
- Petersen, N. O., P. A. Kroon, M. Kainosho, and S. I. Chan. 1975. Thermal phase transitions in deuterated lecithin bilayers. *Chem. Phys. Lipids*. 14:343–349.
- Rietschel, E. T., and H. Brade. 1992. Chemistry of endotoxins. *Sci. Am.* 267:54–61.
- Rietschel, E. T., T. Kirikae, F. U. Schade, U. Mamat, G. Schmidt, H. Loppnow, A. J. Ulmer, U. Zähringer, U. Seydel, F. Di Padova, M. Schreier, and H. Brade. 1994. Bacterial endotoxin: molecular relationships of structure to activity and function. *FASEB J.* 8:217–225.
- Rothschild, K. J., and N. A. Clark. 1979. Polarized infrared spectroscopy of oriented purple membrane. *Biophys. J.* 25:473–488.
- Rottem, S., and L. Leive. 1977. Effects of variation in lipopolysaccharide on the fluidity of the outer membrane of *Escherichia coli*. *J. Biol. Chem.* 252:2088–2081.
- Schletter, J., H. Heine, A. J. Ulmer, and E. T. Rietschel. 1995. Molecular mechanisms of endotoxin activity. *Arch. Microbiol.* 164:383–389.
- Schultz, C. P. 1993. Untersuchungen zur Membran-Organisation lebender Bakterien unter besonderer Berücksichtigung des thermotropen Phasenverhaltens rekonstituierter Lipopolysaccharid-Doppelschichten. Eine Fourier Transform Infrarot-spektroskopische Studie (FT-IR) an Lipopolysacchariden und LPS-Mutanten der Spezies *Salmonella minnesota* und *Salmonella typhimurium*. Ph.D. thesis. Free University Berlin.
- Takeuchi, Y., and H. Nikaido. 1981. Persistence of segregated phospholipid domains in phospholipid-lipopolysaccharide mixed bilayers: studies with spin-labeled phospholipids. *Biochemistry*. 20:523–529.
- Tardieu, A., and V. Luzzati. 1973. Structure and polymorphism of the hydrocarbon chain of lipids: a study of lecithin-water phases. *J. Biol. Chem.* 248:711–733.
- Vaara, M.. 1996. Lipid A: target for antibacterial drugs. *Science*. 274:939–940.
- Vaara, M., and T. Vaara. 1983a. Polycations sensitize enteric bacteria to antibiotics. *Antimicrob. Agents Chemother.* 24:107–113.
- Vaara, M., and T. Vaara. 1983b. Polycations as outer membrane disorganizing agents. *Antimicrob. Agents Chemother.* 24:114–122.
- Wang, S., E. Martin, J. Cimino, G. Omman, and M. Glaser. 1988. Distribution of phospholipid around gramicidin and D-β-hydroxybutyrate dehydrogenase as measured by resonance energy transfer. *Biochemistry*. 27:2033–2039.
- Wiese, A., G. Schröder, K. Brandenburg, A. Hirsch, W. Welte, and U. Seydel. 1994. Influence of the lipid matrix on incorporation and function of LPS-free porin from *Paracoccus denitrificans*. *Biochim. Biophys. Acta.* 1190:231–242.